AUSTRALIAN NETWORK OF STRUCTURAL HEALTH MONITORING

Newsletter

Issue 43, March 2025

Contents

President Report 1
A Universal Smoothing Method for Joint Input-State Estimation of Vibrating Structures 11
Simultaneous Identification of Bridge Properties and Road Roughness from Drive-by Inspection by Integrating Kalman Filter and Optimization Approach 18
Social Media 31

President Message

Tommy Chan

Professor in Civil Engineering, Queensland University of Technology

Dear All,

First of all, a warm welcome to the following new ANSHM members, whose membership applications were approved in the last Executive Committee meeting held on February 13, 2025:

(in the order of application)

1. Mr James Debney of Geomotion Australia
2. Ms Deepti Wagle of V/Line Corporation
3. Dr Yang Zou of The University of Auckland
4. A/Prof Gayan Kahandawa Appuhamillage of Federation University
5. Dr Milad Bazli of Charles Darwin University
6. Dr Ahmed Aseem of ArcStructural

Welcome on board!

I am delighted that we had many applications this time, with three from the industry and three from academia. I believe our industry members can share their SHM experiences in our Newsletter and help us better understand the industry's needs in this area. In our last Advisory Board Meeting (ABM), it was decided to extend our membership to New Zealand.

At our last Advisory Board Meeting (ABM), we decided to extend our membership to New Zealand. Since the revision of the Australian Standards is also applicable to New Zealand, we can consider New Zealand to be part of us. Dr Yang Zou eagerly joined ANSHM once he learned about our new membership policy. We also noted that we have members from nearly all universities in Australia with Civil Engineering disciplines/Schools/Departments, except for five remaining institutions. One of our tasks this year is to identify and approach relevant academics from these five universities to join ANSHM. With the efforts of Prof Brian Uy, we were able to approach Gayan and Milad respectively at Federation University and Charles Darwin University.

Once again, Ahmed, Deepti, Gayan, James, Milad, Yang,
Welcome on board!

In February, Wilson Howe, the President and CEO of Symro (a Canadian SHM technology company specializing in IoT vibration sensing technology), visited Australia as part of a Canadian Trade Delegation. They held a series of priority sector programming meetings in Sydney (February 17-18) and Melbourne (February 20-21). His initial focus is on engaging with Australian engineering firms and potentially exploring research collaborations over time. I am pleased that one of his identified tasks in Australia is to learn more about ANSHM and explore connections and collaborations with us. Our Advisory Board Members, Peter Runcie of NSSN, Govinda Pandley of Rockfield, and John Vazey of EngAnalysis, have already met with Wilson representing ANSHM to introduce him to our work. He is very interested in building a presence in Australia.

Canada can be considered one of the pioneering countries in promoting SHM technology. Prof Aftab Mufti, a Member of the Order of Canada since 2010, has been actively promoting SHM technology as the founding President of the International Society for Structural Health Monitoring of Intelligent Infrastructure (ISHMII), a non-profit organization with global representation. We look forward to a closer connection with Symro through Wilson. If our ARC Research Hub for Sustainable Smart

Infrastructure through Digital Transformation (SSI Hub) grant application is successful, it would be great if Symro can become an Industry Partner of the Hub.

Regarding the Hub application, I am pleased to inform you that we received the Assessor Report with their comments on our 400-page application on February 7, 2025. After receiving the report, we had about two weeks to write the Rejoinder. It is encouraging that two assessors strongly supported the proposal with very positive comments, while the other two assessors provided a mix of positive and negative comments. With the efforts of the Key CIs, Prof Hong Guan of Griffith University, Prof Bijan Samali of Western Sydney University, Prof Brian Uy of the University of New South Wales, and Prof Daoyi Dong of Australian National University, along with constructive suggestions from the other CIs and the assistance of Dr Ronan Nguyen, DECRA, QUT, we crafted a rejoinder within the 5,000-character limit and submitted it to ARC by the deadline of February 20, 2025. Thanks to the combined efforts of the Key CIs and Ronan, we consider the final version to be of very high quality and thoroughly addressing the comments. We hope that the ARC panel will recognize the value of the Hub and award us the grant. The outcome will be announced in July or August later this year.

Below are the updates for the month.

First Executive Committee Meeting in 2025

Our first Executive Committee Meeting of 2025 was held on February 13, 2025. Based on the tasks identified during the discussions at the last Advisory Board Meeting (ABM) on November 21, 2024, and the last Annual General Meeting (AGM) on November 22, 2024, we have reviewed and allocated the roles and duties of the Executive Committee members for the year 2025 as follows:

- Prof Tommy Chan (President): Tommy will continue to lead and chair the Executive Committee and the Advisory Board, working on tasks identified during the discussions at the last ABM and AGM. He will plan for ANSHM to achieve its aims and objectives. If the ARC SSI Hub is announced as successful in July or August, he will become the Director of the Hub. He anticipates being able to manage both roles effectively, with detailed arrangements to be discussed in the Executive Committee meetings after the announcement and the upcoming Advisory Board Meeting in November during the 17th ANSHM Workshop.
- Prof Jianchun Li of UTS (Deputy President): Jianchun will continue working on the Who's Who and research collaborations. He will also contribute to the ITRH scheme if successful.
- Dr Ali Hadigheh of USyd (Industry Coordinator, Academic): As our new Executive Committee member, Ali will share the work with John as Industry Coordinator (Industry). His tasks

include updating the membership database to identify and encourage industry members to contribute to ANSHM, e.g., articles for the Newsletter and presentations for workshops.

- Dr Andy Nguyen of USQ (External Affairs Coordinator): Andy will continue managing ANSHM's external affairs. He aims to create a task force to increase connections and linkages between academics and industry. Additionally, Andy will assist in gathering papers from academics for the Newsletter.
- Prof Alex Ng of the University of Adelaide (Membership Officer): Alex will continue to be the Membership Officer, overseeing all membership matters. With Ali's assistance, he will improve and manage the ANSHM membership database. He will also work with Lei to review ANSHM Rules, especially regarding voting issues.
- A/Prof Colin Caprani of Monash University (SHM Specification Development): Colin will continue working with Ulrike and John on preparing the SHM specifications/guidelines. He will also assist Alex and Ali in managing the ANSHM membership database.
- Prof Hong Guan of Griffith University (ANSHM Website Manager): Hong will continue to manage, update, and upgrade the ANSHM website.
- Mr. John Vazey of EngAnalysis (Industry Coordinator): John will lead the organizing of the upcoming ANSHM workshop. He will continue working as Industry Coordinator (Industry) alongside Ali. Both will work with other EC members to increase industry participation in ANSHM activities.
- A/Prof Lei Hou of RMIT (Web Forum & Social Media Coordinator): Lei will work on a special issue in a high-impact journal as a publication of papers from the 15th and 16th ANSHM Workshops, together with Tommy and the organsiers of the 16th ANSHM Workshop, Dr Govinda Pandey of Rockfield and Prof Rabin Tuladhar of CQU. He will also organize more web forums and promote ANSHM through Facebook, LinkedIn, and YouTube channels. Additionally, he will work with Alex on reviewing the ANSHM Rules on membership matters.
- Prof Jun Li of Curtin University (Newsletter Editor and ANSHM Who's Who): Jun will continue as an editor of the Newsletter and support ANSHM special sessions/symposiums. He will also work with Jianchun on ANSHM Who's Who.
- Dr Mehrisadat Makki Alamdari of UNSW (ANSHM Newsletter Editor): Mehri will continue her role as Newsletter Editor, working with Richard and Jun. She will also work on Technical Notes with Xinqun.
- Prof Richard Yang of UWS (Technical Workshop Coordinator and Newsletter Editor): Richard will continue as part of the editorial team and is happy to organize other training/technical workshops.
- Prof Tuan Ngo of the University of Melbourne (Research Collaboration): Tuan will work with the Research Collaborating Task Force to promote research collaboration within ANSHM.

- Dr Ulrike Dackermann of UNSW (Workshop Coordinator and SHM Specification

Development): Ulrike will continue as the workshop coordinator and assist John in organizing the 17th ANSHM Workshop this year. She will refine and finalise the ANSHM Workshop Sponsorship Guidelines and the Hosting Guidelines for ANSHM Workshops. Additionally, she will contribute to the ANSHM Specifications and provide guidelines specifically for workshop organizers from the industry.

- A/Prof Xinqun Zhu of UTS (Technical Note Coordinator and Technical Workshop Coordinator): Xinqun will continue organizing technical workshops and preparing technical notes.

Video Proceedings for 16th ANSHM Workshop

Many thanks to A/Prof Lei Hou for uploading the video recordings of the 16th ANSHM Workshop to the ANSHM Channel on YouTube. Below are the YouTube links to the recordings for which we have received presenter consent so far. The Video Proceedings for this Workshop will be available on our ANSHM website.

1. ANSHM Vision, Journey and Future Directions by Prof Tommy Chan (ANSHM President, QUT)
2. The 1960s Bridge – Experience and Lessons by Dr Desiree Nortje (Principal Asset Manager, Transurban)
3. Actionable Insights from Bridge Monitoring by Dr Govinda Pandey (CEO, Rockfield Technologies)
4. Synchronisation of Wireless Nodes by A/Prof Colin Caprani (Monash University)
5. Industry Challenges and Visions by John Vazey (Engineering Manager, EngAnalysis)
6. Insights from a Combined BWIM & SHM System by William Macdonald (Mechanical Engineer, EngAnalysis)
7. SHM Facilitating Community Value by Thomas Kuen (Manager Asset Management Research, Melbourne Water)
8. Dynamic Load Allowance using Output-only Methods by Dr David Lo Jacono (ANZ Technical Director, Jacobs)
9. Classification of Steel Corrosion Deterioration by Multispectral Imaging by Dr Rina Hasuike (Yamaguchi University)
10. Integrating IOT and smart Sensor Networks in SHM along with a Case Study by Arend Wieringa (Head of Products and Engineering, Bestech)
11. Advanced Signal Processing and Machine Learning for Damage Detection of Wooden Structure by Dr Mahbube Subhani (Deakin University)
12. Digital Twin Development for Intelligent Monitoring and Maintenance of Concrete Bridges by

Dr Mojtaba Mahmoodian (RMIT University)

13. Rapid In-flight Image Quality Check for UAV-enabled Bridge Inspection by Dr Yang Zou (University of Auckland)
14. Improving Productivity of Infrastructure Projects using Digital Twins and AI Technologies by Prof Tuan Ngo (University of Melbourne)
15. Generative AI Techniques for Structural Health Monitoring by Prof Jun Li (Curtin University)
16. Transfer Learning-based Condition Assessment of Bridges under Moving Vehicles by Prof Jianchun Li (UTS)
17. Deep Learning Computer Vision for Concrete/Pavement Crack Quantification using Information Fusion by Dr Yancheng Li (UTS)
18. Condition Assessment of Plastic Pipes through the Calibration of Frequency-dependent Wave Speed and Attenuation by Dr James Gong (Deakin University)
19. Smart Structural Health Monitoring using Computer Vision and Edge Computing by Dr Zhen Peng (Curtin University)
20. Building Health Monitoring Pattern Identification through Graph Deep Learning by Sajith Wettewa (RMIT University)
21. Integrating Graph Neural Networks and Hybrid Autoencoders for Structural Damage Classification in a Bridge Structure by Syed Haider Mehdi Rizvi (QUT)
22. Investigation of Synchronised LoRa Sensor Nodes for Footbridge Modal Identification by Huiyue Qiao (Griffith University)
23. Panel Discussion: Industry Challenges on SHM
    Panel Members: A/Prof Colin Caprani (Monash University) / Dr Desiree Nortje (Transurban)/ Thomas Kuen (Melbourne Water) / Dr Yew-Chin Koay (Major Road Projects Victoria)
24. Closing Ceremony

17th ANSHM Workshop

The 17th ANSHM Workshop to be held in Newcastle. The organising committee is currently as follows:

- John Vazey (EngAnalysis) Industry Host
- Igor Chaves (UoN) Uni Host
- Desiree Nortje (Transurban)
- Collin Caprani (Monash)
- Ulrike Dackermann (UNSW)

The organising committee has proposed November 20-21, 2025 (tentatively), for the Workshop. They will confirm the availability of ANSHM Executive Committee and Advisory Board members for these dates. The call for presentations will be announced soon.

More details will be provided in upcoming updates.

Special Issue in Journal of Civil Structural Health Monitoring (CSHM)

I am pleased to let you know that the ANSHM special issue will be published in the Feb/March 2025 as a combined special issue of two special issues (topics). The forward of this Special Issue can be accessed online (https://link.springer.com/article/10.1007/s13349-025-00930-0#Sec3). Please see below the Preface for the ANSHM Special Issue of "Digital transformation and intelligent infrastructure for CSHM in Australia".

This special issue pertains to the contributions of Australian and other experts in structural monitoring regarding Digital Transformation and Intelligent Infrastructure for CSHM. After a rigorous peer review and revision, 12 papers were accepted and included in this special issue. These papers address various topics relevant to computer vision-based structural health monitoring, machine learning-based structural condition assessment, advanced non-destructive evaluation techniques, and structural damage identification with limited measurements. As the guest editors of this special issue, we thank the authors who willingly submitted their high-quality work to organize this special issue. The hard work of the reviewers is greatly appreciated, and their valuable comments and suggestions contributed significantly to improving the contents of this special issue.

Academic-Industry Collaboration News

This month marked the successful setup of the research co-location for our EC member, Dr Andy Nguyen from the University of Southern Queensland (UniSQ), with the Queensland Department of

Transport and Main Roads (QDTMR) as part of his Advance Queensland Industry Research Fellowship project, spanning from 2024 to 2027. The research aims to develop effective AI-powered condition monitoring technology for Queensland's key tunnel and bridge structures. This industry research project has been facilitated by Dr Torill Pape and Evan Lo, both long-time ANSHM members, along with their team. Below is a photo from a recent meeting of the project team at QDTMR's Metropolitan office building at 313 Adelaide Street, Brisbane City.

Photo 1: Recent project team meeting, from L to R: Mohamed Nooru-Mohamed (QDTMR), Evan Lo (QDTMR),
Andy Nguyen (UniSQ), and Allan Manalo (UniSQ)

2025 Australian ISWIM Bridge Weigh-in-Motion Workshop Hosted by EngAnalysis

As mentioned in the last monthly update, John Vazey of EngAnalysis, our Industry Liaison Officer (also a member of ANSHM Advisory Board) is organising a one-day workshop on Bridge-Weigh-in-Motion (BWIM) on the trailing end of the Austroads Bridge Conference in June 2025. This workshop is presented in conjunction with the International Society for Weigh in Motion workshop, and the Australian Network of Structural Health Monitoring (ANSHM). The details are given below.

Date:
Saturday 28th of June 2025 – 1 day event

Location:
Rydges Fortitude Valley, Brisbane, 601 Gregory Terrace, Bowen Hills QLD 4006

A roundtable meeting of experts to exchange understandings, explore progress, and connect with people who want to improve bridge asset management through measurement and monitoring.

Guest presenter & global expert:
Dr Aleš Žnidarič (ISWIM Director) will present his experience and a short tutorial on using WIM and bridge WIM data for improved bridge assessment and European perspectives and vision for bridge WIM and bridge monitoring.

Workshop Chairperson: – Chris Koniditsiotis (ISWIM Director) will facilitate the event, guiding the participants through the round-table agenda.

Round Table Agenda:

- Opening – Scene setting
- Presentation from Dr Aleš Žnidarič
- Facilitated round table discussion
- Local Australian projects and initiatives
- Problem identification - Skilled labor, Specialist gear, silo's of expertise, overstated outcomes.
- Vision - Virtual WIM, sharing data, enforcement, privacy
- Technical issues - complex bridges, frequency domain analysis, sensing systems, when influence lines don't really work, what details matter, damage detection.
- Sensor availability - Piezometers, strain, fibre-based, sensing systems

- Commercial and contractual issues - Value, cost, research, collaborations

Tickets are available at:
https://www.trybooking.com/CYTWH
The ticket covers venue access and catering.

Background reading:
https://www.is-wim.net/wp-content/uploads/2024/06/ISWIM_WIM-Data-for-Bridge-Engineering_web_pages_2024.pdf

In the next sections, we will have two articles from our members. The first article is from The University of Sydney on developing a universal smoothing method for joint-state estimation of vibrating structures and the second paper from UNSW on simultaneous identification of bridge properties and road roughness from drive-by inspection by integrating Kalman filter and optimization approach.

With kind regards,
Prof Tommy Chan
President, ANSHM
www.ANSHM.org.au

Professor Tommy H.T. Chan PhD, ThM, MDiv, BE (Hons I), FIEAust, CPEng, NER, APEC Eng, IntPE (Aus), FHKIE, RPE, MICE, C Eng, MCSCE
President ANSHM (www.ANSHM.org.au)
School of Civil & Environmental Engineering, Queensland University of Technology (QUT) GPO Box 2434, Brisbane, QLD 4001, AUSTRALIA.
Ph. +61 7 3138 6732; Fax. +61 7 3138 1170; email: tommy.chan@qut.edu.au;

AUSTRALIAN NETWORK OF STRUCTURAL HEALTH MONITORING
Newsletter

A Universal Smoothing Method for Joint Input-State Estimation of Vibrating Structures

Zihao Liu, Mohsen Ebrahimzadeh Hassanabadi, Daniel Dias-da-Costa*

School of Civil Engineering, The University of Sydney, Sydney, NSW 2006, Australia
Email: daniel.diasdacosta@sydney.edu.au

Abstract
Recursive Bayesian filters are widely used in structural system identification. However, filtering, as an instantaneous system inversion approach, can suffer from ill-conditioning due to sensor network limitations. To address the ill-conditioning of filters, a recursive smoothing algorithm is introduced here for simultaneous input and state estimation of linear systems. Unlike existing minimum-variance unbiased (MVU) smoothing methods, which are constrained by system feedthrough properties, the proposed method is universally applicable to linear systems with or without direct feedthrough and those with rank-deficient feedforward matrices. It also operates without prior knowledge of input statistics. Numerical validations on an eight-storey shear frame and the Taipei 101 tower demonstrate significant improvements over other state-of-the-art methods. The incorporation of singular value truncation further enhances estimation accuracy.

Keywords: structural system identification, structural health monitoring, recursive smoothing method, minimum-variance unbiased estimator, weighted least squares

1. Introduction

Recursive Bayesian filters, such as the Kalman filters and MVU filters [1-4], are widely used in structural health monitoring for estimating the state of linear systems. However, these instantaneous state and input estimation methods can only use the data observed at a single timestep. As a result, system inversion may become ill-conditioned, which can adversely impact the estimation quality. Ill-conditioning can arise due to various factors, including a limited number of sensors, displacement-only or strain-only observations, and non-collocated sensor networks. To remedy this issue, smoothing algorithms extend the observation window. By doing so, smoothing algorithms can benefit from extra sensory information ahead for estimating the state and input, therefore leading to an improved quality of the estimation. This paper introduces a novel recursive smoothing algorithm

for joint input-state estimation of a linear structural system. Based upon a new mathematical formulation, the proposed algorithm is universally applicable to any linear system, regardless of feedthrough properties. For ease of reference, the algorithm is here called Universal Smoothing (US).

2. Overview of the Universal Smoothing

The formulation of the proposed US is briefly introduced in this section. The discrete-time process equation of a linear structural system subjected to dynamic loads can be defined by:

$$\mathbf{x}_k = \mathbf{A}_{k-1}\mathbf{x}_{k-1} + \mathbf{G}_{k-1}\mathbf{p}_k + \mathbf{w}_k, \quad (1)$$

where $\boldsymbol{x}_k \in \mathbb{R}^n$ is the state vector, $\mathbf{p}_k \in \mathbb{R}^m$ is the dynamic input to the system, $\mathbf{A}_k \in \mathbb{R}^{n\times n}$ and $\mathbf{G}_k \in \mathbb{R}^{n\times m}$ are state and input matrices, respectively. The modelling error is expressed by a zero-mean white noise $\mathbf{w}_k \in \mathbb{R}^n$. The observation equation of the structural system reads as:

$$\mathbf{y}_k = \mathbf{C}_k\mathbf{x}_k + \mathbf{H}_k\mathbf{p}_k + \mathbf{v}_k, \quad (2)$$

where $\mathbf{y}_k \in \mathbb{R}^d$ contains the observed output from the system. The output matrix $\mathbf{C}_k \in \mathbb{R}^{d\times n}$ and feedforward matrix $\mathbf{H}_k \in \mathbb{R}^{d\times m}$ relate the state vector $\boldsymbol{x}_k$ and input vector $\mathbf{p}_k$ to the observation $\mathbf{y}_k$ at the same timestep. The zero-mean white noise $\mathbf{v}_k \in \mathbb{R}^d$ represents the observation noise. By introducing an observation window N ($N = 1, 2, \cdots$) in the system described by Eqs. (1) and (2), an extended observation equation is formulated below:

$$\boldsymbol{y}_k = \boldsymbol{\mathcal{C}}_k\mathbf{x}_k + \boldsymbol{\mathcal{H}}_k\boldsymbol{p}_k + \boldsymbol{\mathcal{D}}_k\boldsymbol{w}_k + \boldsymbol{v}_k, \quad (3)$$

where $\boldsymbol{y}_k \in \mathbb{R}^{(N+1)d}$, $\boldsymbol{p}_k \in \mathbb{R}^{(N+1)m}$, $\boldsymbol{w}_k \in \mathbb{R}^{(N+1)n}$, and $\boldsymbol{v}_k \in \mathbb{R}^{(N+1)n}$ are extended vectors. $\boldsymbol{\mathcal{C}}_k$, $\boldsymbol{\mathcal{H}}_k$ and $\boldsymbol{\mathcal{D}}_k$ are extended system matrices.

Based on the linear system defined above, the proposed smoothing algorithm consists of four main steps. First, as the input is unknown, a biased estimate of the state vector without the contribution of

the input can be obtained based on the information from the previous timestep, i.e.:

$$\hat{\boldsymbol{\chi}}_k = \mathbf{A}_{k-1}\hat{\mathbf{x}}_{k-1}. \tag{4}$$

By comparing Eqs. (1), (3) and (4), t can be seen that the bias is caused by the missing contribution of the input. Thus, the innovation $(\boldsymbol{y}_k - \boldsymbol{C}_k\hat{\boldsymbol{\chi}}_k)$ implicitly defines the input estimate, and the input estimate can be inversely calculated by a gain matrix $\mathbf{M}_k$. The input gain, in fact, minimises the variance of input estimation and can be obtained by weighted least squares. Therefore, with the innovation and input gain, the extended input vector can be estimated as:

$$\hat{\boldsymbol{p}}_k = \mathbf{M}_k(\boldsymbol{y}_k - \boldsymbol{C}_k\hat{\boldsymbol{\chi}}_k). \tag{5}$$

Note that the unbiased minimum variance input estimate $\hat{\mathbf{p}}_k$ can be extracted from the extended input vector $\hat{\boldsymbol{p}}_k$. Next, an a-priori estimate of the state vector can be obtained by including the contribution of the estimated input:

$$\hat{\boldsymbol{x}}_k = \hat{\boldsymbol{\chi}}_k + \mathbf{G}_{k-1}\hat{\mathbf{p}}_k. \tag{6}$$

Finally, an a-posteriori estimate of the state vector can be obtained by adding the contribution of the extended observation with an optimal gain matrix $\mathbf{K}_k$ which minimises the error variance of state estimation:

$$\hat{\mathbf{x}}_k = \hat{\boldsymbol{x}}_k + \mathbf{K}_k(\boldsymbol{y}_k - \boldsymbol{C}_k\hat{\boldsymbol{x}}_k - \boldsymbol{\mathcal{H}}_k\hat{\boldsymbol{p}}_k). \tag{7}$$

The smoothing steps, error propagation and calculations of gain matrices are summarised in Table 1. For detailed derivation, readers can refer to [5].

3. Numerical Validation

A high-rise building – the Taipei World Financial Centre, also known as the Taipei 101 tower – is shown in Fig. 1, and the 3-D finite element model of the Taipei 101 is presented in Fig. 2. The numerical simulation is herein used as the case study. All the nodes are constrained in the Y- and Z-directions, whereas the Rayleigh damping with factors $\alpha = \beta = 0.01$ are taken in the dynamic

analysis.

Table 1 Summary of the Universal Smoothing.

- Input estimation
  1. $\boldsymbol{\Gamma}_k = \mathcal{C}_k \mathbf{A}_{k-1}$
  2. $\boldsymbol{\Sigma}_k \triangleq \left[\boldsymbol{\Gamma}_k \quad \breve{\mathbf{D}}_k \quad \mathbf{I}_{(N+1)d}\right]$
  3. $\tilde{\mathbf{R}}_k = \boldsymbol{\Sigma}_k \boldsymbol{\Lambda}_k \boldsymbol{\Sigma}_k^T$
  4. $\mathbf{P}_k^{\boldsymbol{p}} = \left(\breve{\mathbf{H}}_k^T \tilde{\mathbf{R}}_k^{-1} \breve{\mathbf{H}}_k\right)^{-1}$
  5. $\mathbf{P}_k^{\mathbf{p}} = \varepsilon_m \mathbf{P}_k^{\boldsymbol{p}} \varepsilon_m^T$
  6. $\mathbf{M}_k = \mathbf{P}_k^{\boldsymbol{p}} \breve{\mathbf{H}}_k^T \tilde{\mathbf{R}}_k^{-1}$
  7. $\hat{\boldsymbol{\chi}}_k = \mathbf{A}_{k-1} \hat{\mathbf{x}}_{k-1}$
  8. $\hat{\boldsymbol{p}}_k = \mathbf{M}_k \left(\boldsymbol{y}_k - \mathcal{C}_k \hat{\boldsymbol{\chi}}_k\right)$
  9. $\hat{\mathbf{p}}_k = \varepsilon_m \hat{\boldsymbol{p}}_k$
- State estimation
  1. $\hat{\boldsymbol{x}}_k = \hat{\boldsymbol{\chi}}_k + \mathbf{G}_{k-1} \hat{\mathbf{p}}_k$
  2. $\mathbf{V}_k \triangleq \mathbf{G}_{k-1} \varepsilon_m \mathbf{M}_k$
  3. $\mathbf{W}_k \triangleq -\mathbf{V}_k \breve{\mathbf{D}}_k + \varepsilon_n$
  4. $\breve{\mathbf{A}}_{k-1} \triangleq \mathbf{A}_{k-1} - \mathbf{V}_k \boldsymbol{\Gamma}_k$
  5. $\boldsymbol{\Pi}_k \triangleq \left[\breve{\mathbf{A}}_{k-1} \quad \mathbf{W}_k \quad -\mathbf{V}_k\right]$
  6. $\mathbf{P}_k^{\boldsymbol{x}} = \boldsymbol{\Pi}_k \boldsymbol{\Lambda}_k \boldsymbol{\Pi}_k^T$
  7. $\boldsymbol{\Theta}_k = \mathcal{H}_k \mathbf{M}_k$
  8. $\boldsymbol{\Omega}_k \triangleq \left[\mathcal{C}_k \breve{\mathbf{A}}_{k-1} - \boldsymbol{\Theta}_k \boldsymbol{\Gamma}_k \quad \mathcal{C}_k \mathbf{W}_k - \boldsymbol{\Theta}_k \breve{\mathbf{D}}_k + \mathcal{D}_k \quad -\mathcal{C}_k \mathbf{V}_k - \boldsymbol{\Theta}_k + \mathbf{I}_{(N+1)d \times n}\right]$
  9. $\boldsymbol{\Upsilon}_k = -\boldsymbol{\Omega}_k \boldsymbol{\Lambda}_k \boldsymbol{\Pi}_k^T$
  10. $\boldsymbol{\Phi}_k = \boldsymbol{\Omega}_k \boldsymbol{\Lambda}_k \boldsymbol{\Omega}_k^T$
  11. $\mathbf{K}_k = -\boldsymbol{\Upsilon}_k^T \mathbf{U}_k^T \left(\mathbf{U}_k \boldsymbol{\Phi}_k \mathbf{U}_k^T\right)^{-1} \mathbf{U}_k$
  12. $\hat{\mathbf{x}}_k = \hat{\boldsymbol{x}}_k + \mathbf{K}_k \left(\boldsymbol{y}_k - \mathcal{C}_k \hat{\boldsymbol{x}}_k - \mathcal{H}_k \hat{\boldsymbol{p}}_k\right)$
  13. $\mathbf{P}_k = \mathbf{P}_k^{\boldsymbol{x}} + \mathbf{K}_k \boldsymbol{\Upsilon}_k + \boldsymbol{\Upsilon}_k^T \mathbf{K}_k^T + \mathbf{K}_k \boldsymbol{\Phi}_k \mathbf{K}_k^T$
  14. $\mathbf{T}_k = \mathbf{I}_{(N+1)d \times n} - \mathbf{K}_k \mathcal{C}_k$
  15. $\mathcal{W}_k = \mathbf{T}_k \mathbf{W}_k + \mathbf{K}_k \boldsymbol{\Theta}_k \breve{\mathbf{D}}_k - \mathbf{K}_k \mathcal{D}_k$
  16. $\mathcal{V}_k = -\mathbf{T}_k \mathbf{V}_k + \mathbf{K}_k \boldsymbol{\Theta}_k - \mathbf{K}_k$
  17. $\mathcal{A}_k = \mathbf{T}_k \breve{\mathbf{A}}_{k-1} + \mathbf{K}_k \boldsymbol{\Theta}_k \boldsymbol{\Gamma}_k$
  18. $\mathbf{P}_k^{\mathbf{xw}} = \mathcal{A}_k \mathbf{P}_{k-1}^{\mathbf{xw}} \breve{\varepsilon}_n^T + \mathcal{W}_k \mathcal{Q}_{k,k+1}$
  19. $\mathbf{P}_k^{\mathbf{xv}} = \mathcal{A}_k \mathbf{P}_{k-1}^{\mathbf{xv}} \breve{\varepsilon}_d^T + \mathcal{V}_k \mathcal{R}_{k,k+1}$

(a)

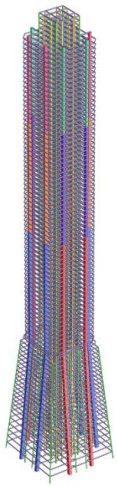

(b)

Figure 1: (a) Taipei 101 tower in Taiwan; (b) the finite element model

To maintain a manageable computational cost despite the dimension and complexity of the structural system, a reduced-order model is adopted. The first fifty natural modes, ranging from 9.981 rad/s

up to 30.633 rad/s, are used to generate dynamic responses under arbitrary load. These results are then contaminated with a zero-mean Gaussian white noise with a level of 5% root-mean-square of the dynamic responses to simulate the observation data. To demonstrate the estimation performance of the US with a rank-deficient feedforward, the model is loaded with two arbitrary excitations acting simultaneously; one is located on an arbitrarily selected column on the 20th floor, and the other one is located on an arbitrarily selected column on the 25th floor. The sensor configuration includes displacement measurements on floors 12, 24, 36, 48, 60, 72 and 84; and only one acceleration sensor on floor 54. The rank-deficiency is created by the single acceleration sensor and two unknown inputs. The performance of the proposed US is compared with existing MVU smoothing with direct feedforward, denoted as MVUS-DF [6].

Fig. 2 shows the input and state estimation results using the US and MVUS-DF. In Figs. 2a and 2b, the MVUS-DF cannot adequately estimate the two unknown inputs, whereas the US exhibits a much-enhanced input identification. In addition, the MVUS-DF underestimates the peak velocity and displacement. The US, on the other hand, can provide consistently accurate state estimation, as shown in Figs. 2c and 2d. By comparing the dimensionless error, the proposed US confirms a 92% improvement.

4. Conclusions

A novel unbiased recursive universal smoothing method was developed. The smoothing algorithm is universally applicable to structural systems with different sensor networks. The algorithm can access more observed information than filtering methods by using measured data in an extended observation window, resulting in a better and more consistent estimation quality. The weighted least squares minimised the variance of the input estimation to derive the input gain, and the state gain was obtained by minimising the trace of the error covariance of the state estimation. Unlike existing Kalman-type estimators, the proposed smoothing algorithm does not require any prior knowledge or assumption on the input. The restriction on the rank condition of the feedforward matrix is also relaxed compared to other minimum variance unbiased estimators.

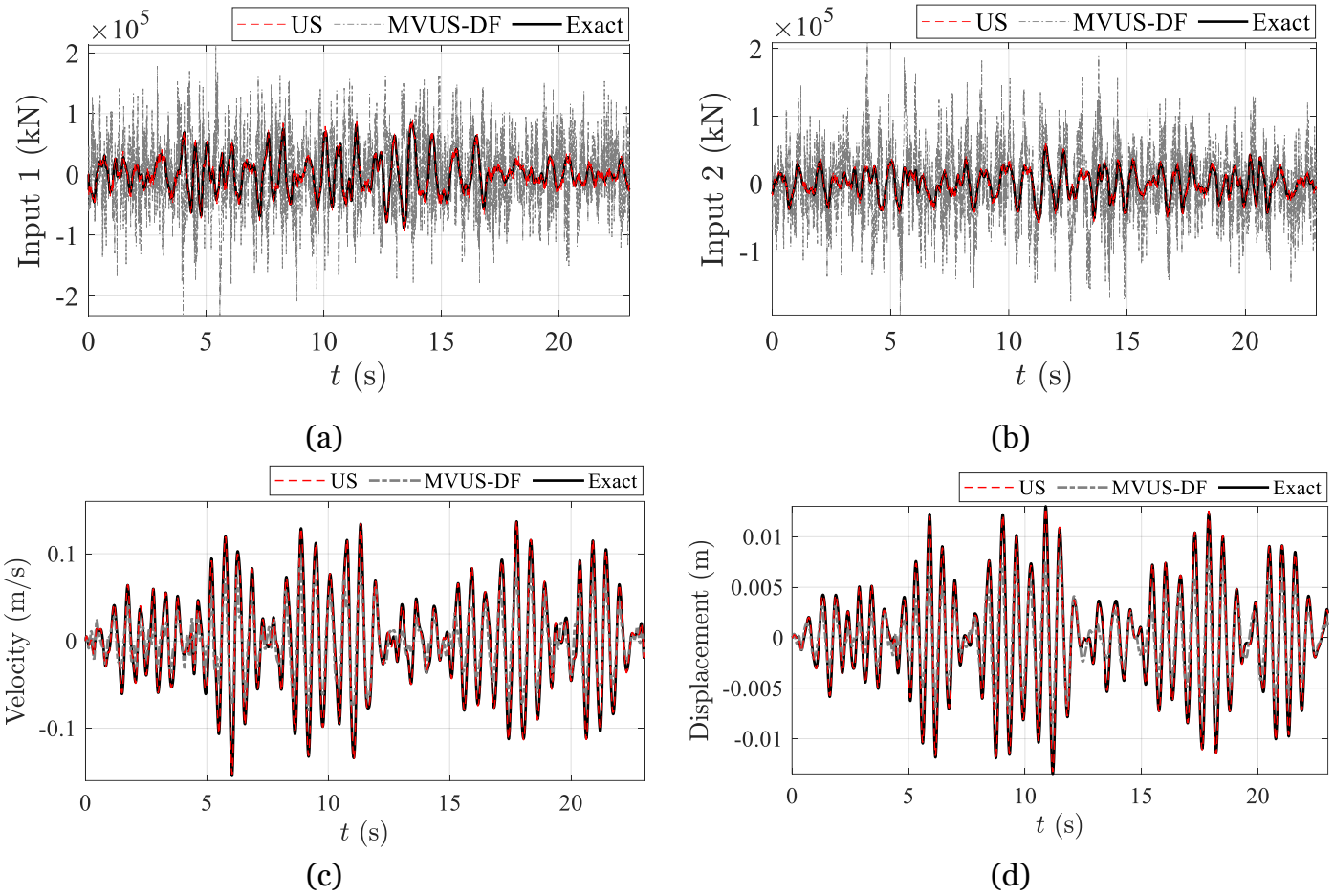

Figure 2: Estimation results: (a) first excitation; (b) second excitation; (c) velocity; and (d) displacement.

In addition, the smoothing algorithm shows numerical stability when deployed to a ROM or a rank-deficient feedforward matrix. The flexibility of the Universal Smoothing suggests its potential as a powerful tool for further deployment in applications such as structural health monitoring, system identification, and the development of digital twins.

Reference

[1] R. E. Kalman, A new approach to linear filtering and prediction problems, Journal of Basic Engineering 82 (1960) 35–45. doi:10.1115/1.3662552.

[2] E. Lourens, E. Reynders, G. De Roeck, G. Degrande, G. Lombaert, An augmented kalman filter for

force identification in structural dynamics, Mechanical Systems and Signal Processing 27 (2012) 446–460. doi:10.1016/j.ymssp.2011.09.025.
[3] S. Gillijns, B. De Moor, Unbiased minimum-variance input and state estimation for linear discrete-time systems, Automatica 43 (2007) 111–116. doi:10.1016/j.automatica.2006.08.002.
[4] S. Gillijns, B. De Moor, Unbiased minimum-variance input and state estimation for linear discrete-time systems with direct feedthrough, Automatica 43 (2007) 934–937. doi:10.1016/j.automatica.2006.11.016.
[5] Z. Liu, M. Ebrahimzadeh Hassanabadi, D. D. da Costa, A linear recursive smoothing method for input and state estimation of vibrating structures, Mechanical Systems and Signal Processing 222 (2025) 111685. doi:10.1016/j.ymssp.2024.111685.
[6] K. Maes, S. Gillijns, G. Lombaert, A smoothing algorithm for joint input-state estimation in structural dynamics, Mechanical Systems and Signal Processing 98 (2018)292–309. doi:10.1016/j.ymssp.2017.04.047.

AUSTRALIAN NETWORK OF STRUCTURAL HEALTH MONITORING
Newsletter

Simultaneous Identification of Bridge Properties and Road Roughness from Drive-by Inspection by Integrating Kalman Filter and Optimization Approach

J. Xu, A. C. Hurtado, E. Atroshchenko, M.M. Alamdari*
Centre for Infrastructure Engineering and Safety, School of Civil and Environmental Engineering, University of New South Wales, Sydney, NSW 2052, Australia
* E-mail: m.makkialamdari@unsw.edu.au

Abstract
In recent decades, researchers have investigated various methodologies for identifying bridge properties through drive-by bridge inspection. However, road roughness has been identified as a crucial component in introducing significant noise into vehicle bridge interaction systems. This work develops two novel strategies to integrate road roughness estimation with vehicle-bridge interaction (VBI) system identification. The proposed approach integrates the Joint-Input-State Kalman Filter with the Particle Swarm Optimisation to identify road roughness and bridge properties simultaneously. The first strategy applies a cooperative identification approach using lightweight and heavyweight sensing vehicles, where the PSO algorithm minimises discrepancies in estimated road roughness profiles to identify bridge stiffness. The second strategy utilises a rigid bump with known geometry at the bridge, formulating an objective function based on deviations between estimated and actual bump properties. The findings confirm that these two strategies achieve reliable results in stiffness identification.

Keywords: Joint-Input-State Kalman Filter; System Identification; Drive-by Bridge Inspection; Structural Health Monitoring

1. Introduction

Indirect Bridge Health Monitoring (IBHM) [1] has gained significant attention due to its ability to extract bridge information from vehicle responses without requiring on-structure sensors [2]. Existing methods primarily focus on identifying bridge modal features, such as natural frequencies [3–5] and mode shapes [6–8], which are useful for structural assessment [9,10]. However, modal parameters alone are insufficient to fully describe the bridge's dynamic behaviour [11]. Since structural integrity is closely related to stiffness, direct stiffness identification is critical for damage detection and service life evaluation [12]. A major challenge in IBHM is the influence of road

roughness, which disturbs vehicle responses and complicates bridge parameter identification. Existing two-stage approaches attempt to decouple road roughness and bridge response using techniques such as the Extended Kalman Filter with Unknown Inputs (EKF-UI) [13] and Augmented Kalman Filter (AKF) [14], but field tests have shown discrepancies between estimated and actual bridge responses [14]. A potential approach to improve decoupling performance is to incorporate vehicle and bridge dynamics into a state-space model, treating bridge displacements as state variables and road roughness as an unknown input. However, the Joint-Input-State Kalman Filter (JISKF) has not yet been applied to road roughness estimation while considering bridge dynamics.
To address these limitations, this study proposes a hybrid methodology that integrates JISKF with Particle Swarm Optimization (PSO) to simultaneously estimate road roughness and bridge stiffness. By leveraging vehicle and bridge interactions within a unified state-space representation, the proposed approach enhances structural parameter identification, overcoming challenges caused by road roughness-induced uncertainties.

2. Joint-Input-State Kalman Filter

To introduce the JISKF [15], a standard discrete time-variant state-space model is used, as given in Equation (1).

$$\begin{aligned} \mathbf{x}_{k+1} &= \mathbf{A}_k\mathbf{x}_k + \mathbf{G}_k\mathbf{u}_k + \mathbf{w} \\ \mathbf{y}_k &= \mathbf{C}_k\mathbf{x}_k + \mathbf{H}_k\mathbf{u}_k + \mathbf{v} \end{aligned} \tag{1}$$

where $\mathbf{A}_k$ represents a time-variant state transition matrix. $\mathbf{u}_k$ is the input of the system. $\mathbf{G}_k$ is the system input matrix, which defines how the system input influences the system state. $\mathbf{w}$ is the zero-mean Gaussian white noise with covariance matrix $\mathbf{Q}$, used to reflect the uncertainty of the system model. The measurement equation is shown in a feed-through form in Equation (1), in which the measurement has a direct relation with the input $\mathbf{u}_k$. $\mathbf{C}_k$ is the output matrix, and $\mathbf{H}_k$ is called the feed-through matrix. $\mathbf{v}$ is also a zero-mean Gaussian white noise with covariance matrix $\mathbf{R}$.

For the implementation of JISKF [15], the required parameters are defined. $\hat{\mathbf{x}}_k$ is the estimated state

vector, and $\hat{\mathbf{u}}_k$ is the estimated unknown input. The state error covariance matrix $\mathbf{P}_{x,k|k}$ quantifies the uncertainty in state estimation while $\mathbf{P}_{u,k}$ represents the error covariance of the estimated input. $\mathbf{P}_{xu,k}$ is the cross-covariance between state and input estimation errors, with $\mathbf{P}_{ux,k}$ as its transpose. $\mathbf{\Phi}_k$ is the innovation covariance, as defined in [15]. $\mathbf{\Sigma}_k$ and $\mathbf{\Upsilon}_k$ denote the input and state estimation gain matrices, respectively. The initial state vector initialises the JISKF $\hat{\mathbf{x}}_{0|-1}$ and initial error covariance matrix $\mathbf{P}_{x,0|-1}$ [15]. Once the JISKF is initialised, a three-stage process is followed: (1) Input estimation, (2) Measurement update and (3) Time update. At each time step, Equations (2) to (11) are iteratively applied, and the estimated values of $\hat{u}_k$ are recorded to obtain the estimate of the unknown input over time.

Input estimation:

$$\mathbf{\Phi}_k = \mathbf{C}_k \mathbf{P}_{x,k|k-1} \mathbf{C}_k^T + \mathbf{R} \tag{2}$$

$$\mathbf{\Sigma}_k = (\mathbf{H}_k^T \mathbf{\Phi}_k^{-1} \mathbf{H}_k)^{-1} \mathbf{H}_k^T \mathbf{\Phi}_k^{-1} \tag{3}$$

$$\hat{\mathbf{u}}_k = \mathbf{\Sigma}_k (\mathbf{y}_k - \mathbf{C}_k \hat{\mathbf{x}}_{k|k-1}) \tag{4}$$

$$\mathbf{P}_{u,k} = (\mathbf{H}_k^T \mathbf{\Phi}_k^{-1} \mathbf{H}_k)^{-1} \tag{5}$$

Measurement update:

$$\mathbf{\Upsilon}_k = \mathbf{P}_{x,k|k-1} \mathbf{C}_k^T \mathbf{\Phi}_k^{-1} \tag{6}$$

$$\hat{\mathbf{x}}_{k|k} = \hat{\mathbf{x}}_{k|k-1} + \mathbf{\Upsilon}_k (\mathbf{y}_k - \mathbf{C}_k \hat{\mathbf{x}}_{k|k-1} - \mathbf{H}_k \hat{\mathbf{u}}_k) \tag{7}$$

$$\mathbf{P}_{x,k|k} = \mathbf{P}_{x,k|k-1} - \mathbf{Y}_k(\mathbf{\Phi}_k - \mathbf{H}_k\mathbf{P}_{u,k}\mathbf{H}_k^T)\mathbf{Y}_k^T \tag{8}$$

$$\mathbf{P}_{xu,k} = \mathbf{P}_{ux,k}^T = -\mathbf{Y}_k\mathbf{H}_k\mathbf{P}_{u,k} \tag{9}$$

Time update:

$$\hat{\mathbf{x}}_{k+1|k} = \mathbf{A}_k\hat{\mathbf{x}}_{k|k} + \mathbf{G}_k\hat{\mathbf{u}}_k \tag{10}$$

$$\mathbf{P}_{x,k+1|k} = [\mathbf{A}_k\ \mathbf{G}_k]\begin{bmatrix}\mathbf{P}_{x,k|k} & \mathbf{P}_{xu,k}\\ \mathbf{P}_{ux,k} & \mathbf{P}_{u,k}\end{bmatrix}\begin{bmatrix}\mathbf{A}_k^T\\ \mathbf{G}_k^T\end{bmatrix} + \mathbf{Q} \tag{11}$$

3. VBI system

The quarter-car VBI model is used in this study to represent the interaction between a moving vehicle and a bridge with road roughness. The governing Equation of the quarter-car VBI system is defined as Equation (12).

$$\mathbf{M}_{vb}\ddot{\mathbf{z}}_{vb}(t) + \mathbf{C}_{vb}\dot{\mathbf{z}}_{vb}(t) + \mathbf{K}_{vb}\mathbf{z}_{vb}(t) = \mathbf{F}_{vb}(t) \tag{12}$$

where $\mathbf{M}_{vb}$, $\mathbf{K}_{vb}$ and $\mathbf{C}_{vb}$ represent the coupled mass, stiffness, and damping matrices for the VBI system, which can be found in Equation (A1) in the Appendix. These matrices have a size of $N_{vb} \times N_{vb}$, where $N_{vb} = N + 2$, with N representing the DOF of the bridge and the additional two accounts for the DOF of the vehicle. $\mathbf{z}_{vb}(t)$, $\dot{\mathbf{z}}_{vb}(t)$, and $\ddot{\mathbf{z}}_{vb}(t)$ represents the displacement, velocity, and acceleration vectors of the VBI system, along with the force vector $\mathbf{F}_{vb}(t)$ are defined in Equation (A2). Equation (12) could be solved by the Newmark-beta method to obtain the displacement and acceleration response of the vehicle and tyre. The bridge properties used in this study are listed in Table 1, where the bridge is modelled as a simply supported beam. The vehicle is considered to travel at a constant speed of 2m/s while crossing the bridge. 10% Gaussian white noise is added to the measured acceleration response to simulate the measurement noise.

Table 1: Bridge properties.

L [m]	25
A [m^2]	3.2
I [m^4]	0.171
ρ [kg/m^3]	4,800
E [Pa]	2.75×10^{10}
ζ[%]	3%

4. Strategy I: Cooperative Identification with Lightweight and Heavyweight Sensing Vehicles

This strategy employs a Lightweight Sensing Vehicle (LSV) and a Heavyweight Sensing Vehicle (HSV) to estimate road roughness and identify bridge stiffness *EI*. The LSV first estimates the road roughness profile $\hat{\mathbf{u}}_L$ using the JISKF framework described in Section 2, treating road roughness profile as the unknown input while assuming negligible VBI dynamic due to its low mass. This estimated $\hat{\mathbf{u}}_L$ serves as a reference for HSV. The state-space representation for LSV is described in Equation (13).

$$\begin{aligned} \mathbf{x}_{L,k+1} &= \mathbf{A}_L\mathbf{x}_{L,k} + \mathbf{G}_L\mathbf{u}_{L,k} + \mathbf{w} \\ \mathbf{y}_{L,k} &= \mathbf{C}_L\mathbf{x}_{L,k} + \mathbf{H}_L\mathbf{u}_{L,k} + \mathbf{v} \\ \mathbf{x}_{L,k} = [\mathbf{z}_v(t), \dot{\mathbf{z}}_v(t)]^T, \mathbf{y}_{L,k} &= [z_v - z_t, z_v, \ddot{z}_v, \ddot{z}_t]^T \end{aligned} \tag{13}$$

Since the LSV system matrices $\mathbf{A}_L$, $\mathbf{G}_L$, $\mathbf{C}_L$ and $\mathbf{H}_L$ exclude bridge-related terms, the estimated

roughness profile $\hat{\mathbf{u}}_L$ is only dependent on the vehicle parameters. The state space matrix $\mathbf{A}_L$ of the LSV has a size of $N_L \times N_L$, and $\mathbf{G}_L$ is of size $N_L \times 1$,, where $N_L = 4$. These matrices are defined in Equations (A5) and (A6). The vehicle parameters for LSV are presented in Table 2.

Table 2: LSV properties.

m_v [kg]	25
k_v [N/m]	1.2×10^3
c_v [N.s/m]	32
m_t [kg]	2
k_t [N/m]	5.0×10^3

The VBI dynamic cannot be neglected for the HSV, and its state-space representation is shown in Equation (14).

$$\begin{gathered}\mathbf{x}_{H,k+1} = \mathbf{A}_{H,k}\mathbf{x}_{H,k} + \mathbf{G}_{H,k}\mathbf{u}_{H,k} + \mathbf{F}_{H,k} + \mathbf{w} \\ \mathbf{y}_{H,k} = \mathbf{C}_{H,k}\mathbf{x}_{H,k} + \mathbf{H}_H\mathbf{u}_{H,k} + \mathbf{v} \\ \mathbf{x}_{H,k} = \left[\mathbf{z}_{H,vb}(t), \dot{\mathbf{z}}_{H,vb}(t)\right]^T, \mathbf{y}_{H,k} = [z_v - z_t, z_v, \ddot{z}_v, \ddot{z}_t]^T\end{gathered} \tag{14}$$

Here, the HSV system matrices $\mathbf{A}_{H,k}$ and $\mathbf{G}_{H,k}$ are dependent on the bridge stiffness EI, which is the unknown target parameter to be identified. Therefore, the JISKF procedure could be treated as the function of bridge stiffness EI with the output of $\hat{\mathbf{u}}_H$. The system matrices $\mathbf{A}_{H,k}$, $\mathbf{G}_{H,k}$, $\mathbf{C}_{H,k}$, and $\mathbf{H}_H$ are defined in Equations (A3) and (A4). The state space matrix $\mathbf{A}_{H,k}$ is of size $N_s \times N_s$ and $\mathbf{G}_{H,k}$ is of size $N_L \times 1$, where $N_L = 2 \times N_{vb}$. The vehicle parameters used for the HSV are listed in Table 3.

Table 3: HSV properties.

m_v [kg]	14,000
k_v [N/m]	2×10^5
c_v [N.s/m]	10,000
m_t [kg]	1,000
k_t [N/m]	2.75×10^6

Bridge stiffness is identified by minimising the difference between the estimated roughness profiles $\hat{\mathbf{u}}_{\mathrm{L}}$ and $\hat{\mathbf{u}}_{\mathrm{H}}(EI)$, using the objective function shown in Equation (15).

$$J_{LH}(EI) = \frac{\sum_{i=1}^{n}\left[\hat{u}_{L,i} - \hat{u}_{H,i}(EI)\right]^2}{\sum_{i=1}^{n}\left[\hat{u}_{L,i} - \hat{u}_{L,avg}\right]^2}, \hat{u}_{L,avg} = \frac{1}{n}\sum_{i=1}^{n}\hat{u}_{L,i} \quad (15)$$

Where i denotes the index of discrete points in the road roughness profile, and n is the total number of points along the LSV and HSV trajectories. J_{LH} represents the objective function of the cooperative identification strategy while $\hat{u}_{L,avg}$ is the mean estimated roughness from LSV. The PSO algorithm is applied to iteratively update *EI* until the discrepancy between the road roughness profiles estimated by the LSV and HSV is minimised. The identification performance is quantified by the relative error rate ϵ, which is a percentage.

$$\epsilon = \left| \frac{EI_{\text{est}} - EI_{\text{true}}}{EI_{\text{true}}} \right| \times 100\% \tag{16}$$

5. Strategy II: Artificial Speed Bump-Assisted Identification

The second strategy introduces a rigid speed bump with known dimensions to aid bridge stiffness identification. Since the bump does not deform, its shape appears in the estimated road roughness profile obtained via the JISKF framework. The *EI* is identified by minimising the estimated and actual bump shape discrepancy.

The bump follows a symmetrical half-sine profile, defined as Equation (17).

$$\xi(x) = \begin{cases} h \cdot \sin\left(\dfrac{\pi \cdot (x - x_0 + \frac{l}{2})}{l} \right), & x_0 - \dfrac{l}{2} \le x \le x_0 + \dfrac{l}{2}, \\ 0, & \text{otherwise.} \end{cases} \tag{17}$$

Where $x_0 - \frac{l}{2}$ and $x_0 + \frac{l}{2}$ represent the starting and ending positions of the speed bump while x_0 denotes its center position. The state-space model used in Strategy II is consistent with the one used in HSV, as presented in Equation (14). Since the location of the artificial speed bump is predefined, the estimated bump profile $\hat{r}_{\xi,i}(EI)$ can be isolated from the road roughness profile obtained through the JISKF framework. The objective function is formulated as Equation (18).

$$J_\xi(EI) = \frac{\sum_{i=1}^{n} \left[r_{\xi,i} - \hat{r}_{\xi,i}(EI) \right]^2}{\sum_{i=1}^{n} \left[r_{\xi,i} - r_{\xi,avg} \right]^2}, r_{\xi,avg} = \frac{1}{n} \sum_{i=1}^{n} r_{\xi,i} \tag{18}$$

Here, i indexes the discrete points within the bump profile, and n denotes the total number of

contact points between the bump and the sensing vehicle's tyre. The objective function, J_ξ, corresponds to the optimisation process while $r_{\xi,avg}$ represents the average value of the actual speed bump profile.

6. Results and Discussion

a. Effect of Road Roughness Level on Strategy I

The performance of the *EI* estimation is evaluated under four road roughness levels, Type A to Type D, with 20 independent profiles generated for each type. Assuming the LSV and HSV experience the same roughness, vehicle responses are simulated following Section 3, and *EI* estimation follows Section 4.

Figure 1 presents the relative error distribution, showing consistently low errors below 3%. The mean error rate increases from 0.16% for Type A to 0.76% for Type D, while the standard deviation rises from 0.10% to 0.62%. To assess the variability, the coefficient of variation (Cov) is computed as the standard deviation divided by the mean error, increasing from 0.625 for Type A to 0.816 for Type D. However, even the uncertainty in the identification process increases, Strategy I still achieves satisfactory identification performance.

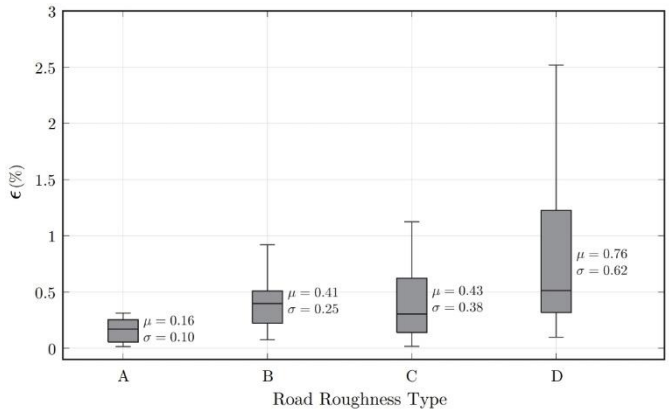

Figure 1: boxplot of relative error rate in *EI* estimates from Strategy I for different road roughness levels.

b. Effect of Speed Bump Position on Strategy II

The optimal speed bump location for EI identification is evaluated at seven positions along the bridge span, with 20 crossings per case. Figure 2 shows the relative error distribution, where the lowest mean error of 0.71% occurs at mid-span with a standard deviation of 0.43%. As the bump moves toward the bridge ends, both values increase, reaching 2.58% mean error and 1.77% standard deviation at 7/8 span. The Cov rises from 0.61 at mid-span to 0.69 at 7/8 span, indicating higher uncertainty when the bump is near the supports. These results suggest that when using the proposed framework, the speed bump is better placed as close to mid-span as possible for optimal performance.

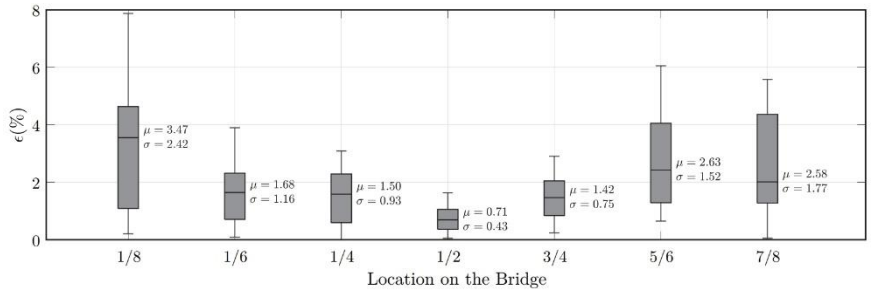

Figure 2: Boxplot of relative error in *EI* estimates from Strategy II for different bump locations.

c. Effect of Speed Bump Position on Strategy II

The effect of speed bump height on EI identification is evaluated for five heights ranging from 1 cm to 5 cm, with 20 crossings per case. Figure 3 presents the relative error distribution, showing that bumps of 1 cm and 2 cm yield the most accurate estimates, with mean errors of 0.34% and 0.26%, both with a standard deviation of 0.24%. As bump height increases, both the mean error and standard deviation become larger, reaching 0.98% mean error and 0.59% standard deviation at 5 cm. It decreases from 0.71 at 1 cm to 0.60 at 5 cm, indicating that while absolute error increases, variability relative to the mean error is slightly reduced for taller bumps. Overall, the results confirm that Strategy II is affected by both bump location and height, with optimal performance achieved when the bump is placed at mid-span and kept at a lower height.

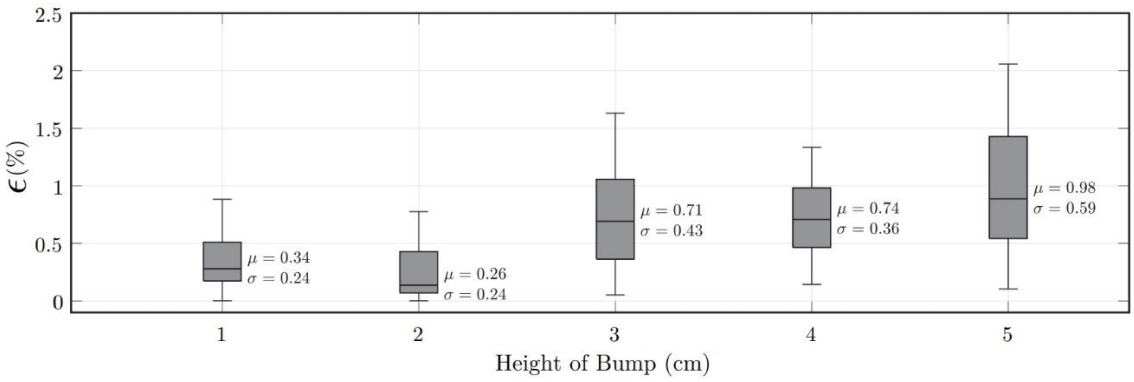

Figure 3: Boxplot of relative error rate in *EI* estimates from Strategy II for different bump heights.

7. Conclusion

This study proposed two strategies for bridge stiffness identification using road roughness estimation. Strategy I used two sensing vehicles, while Strategy II relied on an artificial speed bump. Results showed that both methods achieved reliable *EI* estimation. Strategy I maintained a relative error rate below 3% across different road roughness conditions. In Strategy II, the position and height of the bump influenced identification performance, with the best results obtained when the bump was placed at mid-span and had a lower height. Future work would extend these strategies to advanced VBI models and validate them through experiments.

8. Appendix

$$\mathbf{M}_{vb} = \begin{bmatrix} \mathbf{M}_v & \mathbf{0} \\ \mathbf{0} & \mathbf{M}_b \end{bmatrix}_{N_{vb}\times N_{vb}}, \mathbf{C}_{vb} = \begin{bmatrix} \mathbf{C}_v & \mathbf{0} \\ \mathbf{0} & \mathbf{C}_b \end{bmatrix}_{N_{vb}\times N_{vb}}, \mathbf{F}_{vb}(t) = \begin{bmatrix} 0 \\ k_t r(x_v) \\ -\{\boldsymbol{\iota}_b(x_v)\}\boldsymbol{\Gamma}(t) \end{bmatrix}_{N_{vb}\times 1}, \mathbf{M}_v = \begin{bmatrix} m_v & 0 \\ 0 & m_t \end{bmatrix}, \mathbf{C}_v = \begin{bmatrix} c_v & -c_v \\ -c_v & c_v \end{bmatrix}$$

$$\mathbf{K}_{vb} = \begin{bmatrix} k_v & -k_v & \mathbf{0}_{1\times N} \\ -k_v & k_v + k_t & -k_t\{\boldsymbol{\iota}_b(x_v)\}^T \\ \mathbf{0}_{N\times 1} & -k_t\{\boldsymbol{\iota}_b(x_v)\} & \mathbf{K}_b + k_t\{\boldsymbol{\iota}_b(x_v)\}\{\boldsymbol{\iota}_b(x_v)\}^T \end{bmatrix}_{N_{vb}\times N_{vb}}, \mathbf{K}_v = \begin{bmatrix} k_v & -k_v \\ -k_v & k_v + k_t \end{bmatrix}$$

$$\boldsymbol{N}_b = \left[1 - \frac{3x_e^2}{L_e^2} + \frac{2x_e^3}{L_e^3}, x - \frac{2x_e^2}{L_e} + \frac{x_e^3}{L_e^2}, \frac{3x_e^2}{L_e^2} - \frac{2x_e^3}{L_e^3}, \frac{x_e^3}{L_e^2} - \frac{x_e^2}{L_e}\right]^T, \{\boldsymbol{\iota}_b(x_v)\} = [0,0,\cdots,\boldsymbol{N}_b,\cdots,0,0]^T$$

$$\mathbf{z}_{vb}(t) = \begin{bmatrix} z_v(t) \\ z_t(t) \\ \mathbf{Z}_b(t) \end{bmatrix}_{N_{vb}\times 1}, \dot{\mathbf{z}}_{vb}(t) = \begin{bmatrix} \dot{z}_v(t) \\ \dot{z}_t(t) \\ \dot{\mathbf{Z}}_b(t) \end{bmatrix}_{N_{vb}\times 1}, \ddot{\mathbf{z}}_{vb}(t) = \begin{bmatrix} \ddot{z}_v(t) \\ \ddot{z}_t(t) \\ \ddot{\mathbf{Z}}_b(t) \end{bmatrix}_{N_{vb}\times 1}, \quad (A2)$$

$$\mathbf{A}_{H,k} = \exp\left(\begin{bmatrix} \mathbf{0} & \mathbf{I} \\ -\mathbf{M}_{vb}^{-1}\mathbf{K}_{vb} & -\mathbf{M}_{vb}^{-1}\mathbf{C}_{vb} \end{bmatrix}\Delta t\right)_{N_s\times N_s}, \mathbf{F}_{H,k} = \begin{bmatrix} \mathbf{0} \\ -[\mathbf{M}_b^{-1}(m_v+m_t)g]\{\boldsymbol{\iota}_b(x_v)\} \end{bmatrix}_{N_s\times 1},$$

$$\mathbf{G}_{H,k} = \left((\mathbf{A}_{H,k}-\mathbf{I})\begin{bmatrix} \mathbf{0} & \mathbf{I} \\ -\mathbf{M}_{vb}^{-1}\mathbf{K}_{vb} & -\mathbf{M}_{vb}^{-1}\mathbf{C}_{vb} \end{bmatrix}^{-1}\begin{bmatrix} \mathbf{0} \\ \boldsymbol{\eta}_k \end{bmatrix}\right)_{N_s\times 1}, \mathbf{C}_{H,k} = \begin{bmatrix} \mathbf{S} & \mathbf{0} & \mathbf{0} & \mathbf{0} \\ -\mathbf{M}_v^{-1}\mathbf{K}_v & \boldsymbol{\theta}_k & -\mathbf{M}_v^{-1}\mathbf{C}_v & \mathbf{0} \end{bmatrix}_{N_m\times N_s}, \mathbf{S} = \begin{bmatrix} 1 & -1 \\ 1 & 0 \end{bmatrix} \quad (A3)$$

$$\boldsymbol{\eta}_k = \begin{bmatrix} \frac{k_t}{m_t} \\ -k_t\boldsymbol{M}_b^{-1}\boldsymbol{\iota}_b(x_v) \end{bmatrix}, \boldsymbol{H}_H = \begin{bmatrix} \mathbf{0} \\ \frac{k_t}{m_t} \end{bmatrix}, \boldsymbol{\theta}_k = \begin{bmatrix} \mathbf{0} \\ \frac{k_t}{m_t}\{\boldsymbol{\iota}_b(x_v)\}^T \end{bmatrix} \quad (A4)$$

$$\mathbf{A}_L = \exp\left(\begin{bmatrix} \mathbf{0} & \mathbf{I} \\ -\mathbf{M}_v^{-1}\mathbf{K}_v & -\mathbf{M}_v^{-1}\mathbf{C}_v \end{bmatrix}\Delta t\right)_{N_L\times N_L}, \mathbf{G}_L = \left((\mathbf{A}_L-\mathbf{I})\begin{bmatrix} \mathbf{0} & \mathbf{I} \\ -\mathbf{M}_v^{-1}\mathbf{K}_v & -\mathbf{M}_v^{-1}\mathbf{C}_v \end{bmatrix}^{-1}\begin{bmatrix} \mathbf{0} \\ \frac{k_t}{m_t} \end{bmatrix}\right)_{N_m\times 1} \quad (A5)$$

$$\mathbf{C}_L = \begin{bmatrix} \mathbf{S} & \mathbf{0} \\ -\mathbf{M}_v^{-1}\mathbf{K}_v & -\mathbf{M}_v^{-1}\mathbf{C}_v \end{bmatrix}_{N_m\times N_L}, \mathbf{H}_L = \begin{bmatrix} \mathbf{0} \\ \frac{k_t}{m_t} \end{bmatrix}_{N_m\times 1} \quad (A6)$$

$$\mathbf{z}_L(t) = \begin{bmatrix} z_v(t) \\ z_t(t) \end{bmatrix}, \dot{\mathbf{z}}_L = \begin{bmatrix} \dot{z}_v(t) \\ \dot{z}_t(t) \end{bmatrix}, \ddot{\mathbf{z}}_L(t) = \begin{bmatrix} \ddot{z}_v(t) \\ \ddot{z}_t(t) \end{bmatrix}, \mathbf{F}_L(t) = \begin{bmatrix} 0 \\ k_t r(x_L) \end{bmatrix} \quad (A7)$$

References

[1] Y. Yang and C. Lin, Vehicle–bridge interaction dynamics and potential applications, Journal of Sound and Vibration, vol. 284, no. 1, pp. 205–226, 2005.

[2] Y. B. Yang and J. P. Yang, State-of-the-art review on modal identification and damage detection of bridges by moving test vehicles, International Journal of Structural Stability and Dynamics, vol. 18, no. 02, p. 1850025, 2018.

[3] Y.-B. Yang, W.-F. Chen, H.-W. Yu, and C. S. Chan, Experimental study of a hand-drawn cart for measuring bridge frequencies, Engineering Structures, vol. 57, pp. 222–231, 2013.

[4] P. J. McGetrick, A. González, and E. J. O'Brien, Theoretical investigation of the use of a moving vehicle to identify bridge dynamic parameters, Insight - Non-Destructive Testing and Condition Monitoring, vol. 51, pp. 433–438, 2009.

[5] M. Makki Alamdari, K. Chang, C. Kim, K. Kildashti, and H. Kalhori, Transmissibility performance

assessment for drive-by bridge inspection, Engineering Structures, vol. 242, p. 112485, 2021.
[6] Y. Zhang, S. T. Lie, and Z. Xiang, Damage detection method based on operating deflection shape curvature extracted from dynamic response of a passing vehicle, Mechanical Systems and Signal Processing, vol. 35, no. 1, pp. 238–254, 2013.
[7] Y. Yang, Y. Li, and K. Chang, Constructing the mode shapes of a bridge from a passing vehicle: A theoretical study, Smart Structures and Systems, vol. 13, pp. 797–819, 2014.
[8] Y. Zhang, H. Zhao, and S. T. Lie, Estimation of mode shapes of beam-like structures by a moving lumped mass, Engineering Structures, vol. 180, pp. 654–668, 2019.
[9] Q. Mei, M. Gül, and M. Boay, Indirect health monitoring of bridges using mel-frequency cepstral coefficients and principal component analysis, Mechanical Systems and Signal Processing, vol. 119, pp. 523–546, 2019.
[10] R. Corbally and A. Malekjafarian, A data-driven approach for drive-by damage detection in bridges considering the influence of temperature change, Engineering Structures, vol. 253, p. 113783, 2022.
[11] D. Ewins, Modal Testing: Theory, Practice and Application, 2nd ed. Wiley, 2000.
[12] J. Sinha, M. Friswell, and S. Edwards, Simplified models for the location of cracks in beam structures using measured vibration data, Journal of Sound and Vibration, vol. 251, no. 1, pp. 13–38, 2002.
[13] Y. B. Yang, B. Wang, Z. Wang, K. Shi, and H. Xu, Scanning of bridge surface roughness from two-axle vehicle response by EKF-UI and contact residual: Theoretical study, Sensors, vol. 22, no. 9, 2022.
[14] R. Shin, Y. Okada, and K. Yamamoto, Discussion on a vehicle–bridge interaction system identification in a field test, Sensors, vol. 23, no. 1, 2023.
[15] K. Maes, K. V. Nimmen, E. Lourens, A. Rezayat, P. Guillaume, G. D. Roeck, and G. Lombaert, Verification of joint input-state estimation for force identification by means of in situ measurements on a footbridge, Mechanical Systems and Signal Processing, vol. 75, pp. 245–260, 2016

Conferences News

Special Session at IABSE Tokyo 2025

As mentioned before, Dr Fabien Rollet, and Dr David Lo Jacono, Technical Directors at Jacobs are organising a special session at the International Association for Bridge and Structural Engineering (IABSE) is organising their Symposium in Tokyo at Waseda University and Rihga Royal Hotel from 18 to 21 May 2025 (IABSE - Tokyo 2025), with the support of ANSHM. The theme of the symposium is Environmentally Friendly Technologies and Structures: Focusing on Sustainable Approaches. The Special Session is "SS14: Dynamic Bridge Assessment and Performance". The full papers Acceptance is scheduled to be notified on 18 February 2025. Please notify me if you have submitted papers to this Special Session SS14.

EMI 2025 International Conference, Beijing, China

A/Prof Xinqun Zhu of UTS is organising a min-symposia at EMI 2025 International Conference, Beijing China, July 17-20, 2025. The title of the symposia is "Vehicle-bridge interaction based structural health monitoring". This mini-symposium is designed to showcase the most recent advances in vehicle-bridge interaction-based structural health monitoring for transport infrastructures. They are calling for submissions from academic researchers and industry professionals in fields, such as theoretical modelling, numerical validation, laboratory experiments, and field testing. Members of ANSHM are welcome to submit and present your recent work to our symposia. The details information can be found on the website: https://emi-ic.asce.org/call-abstracts. Please note that the Abstract submission deadline is **3 February 2025**.

12th Austroads Bridge Conference (2025)

The 12th Austroads Bridge Conference will be held in Brisbane, Queensland from 25 – 27 June 2025 (https://austroads.gov.au/webinars-and-events/12th-austroads-bridge-conference-2025).

Social Media

Follow us at the next social media and webpages

- ANSHM Facebook webpage: www.facebook.com/ANSHMAU
- ANSHM Facebook group: www.facebook.com/groups/ANSHM

- ANSHM LinkedIn group:
  www.linkedin.com/groups/ANSHM-Australian-Network-Structural-Health-4965305

Call for Articles

Interested in publishing an article in ANSHM newsletter, please register here
https://docs.google.com/document/d/1XJX9qhxEfIkXSVluWDV5rvROuYySM-hWn-q9n80-Tzw/edit?usp=sharing

Edition	Submission Deadline	Distribution
Spring	15 Feb	Early March
Summer	15 May	Early June
Fall	15 Aug	Early Sep
Winter	15 Nov	Early Dec

If you have any comments and suggestions, please contact

Newsletter Editors:

Dr. Mehrisadat Makki Alamdari, University of New South Wales.

Email: m.makkialamdari@unsw.edu.au

Dr. Jun Li, Curtin University.

Email: junli@curtin.edu.au

Prof. Richard Yang, Western Sydney University.

Email: R.Yang@westernsydney.edu.au